Experimental Study of the Exciton Gas-Liquid Transition in Coupled Quantum Wells

Subhradeep Misra,[1] Michael Stern,[2] Arjun Joshua,[1] Vladimir Umansky,[1] and Israel Bar-Joseph[1,*]
[1]Department of Condensed Matter Physics, Weizmann Institute of Science, Rehovot 7610001, Israel
[2]Institute of Nanotechnology and Advanced Materials, Bar-Ilan University, Ramat-Gan 5290002, Israel

(Received 27 August 2017; published 26 January 2018)

We study the exciton gas-liquid transition in GaAs/AlGaAs coupled quantum wells. Below a critical temperature, $T_C = 4.8$ K, and above a threshold laser power density the system undergoes a phase transition into a liquid state. We determine the density-temperature phase diagram over the temperature range 0.1–4.8 K. We find that the latent heat increases linearly with temperature at $T \lesssim 1.1$ K, similarly to a Bose-Einstein condensate transition, and becomes constant at $1.1 \lesssim T < 4.8$ K. Resonant Rayleigh scattering measurements reveal that the disorder in the sample is strongly suppressed and the diffusion coefficient sharply increases with decreasing temperature at $T < T_C$, allowing the liquid to spread over large distances away from the excitation region. We suggest that our findings are manifestations of a quantum liquid behavior.

DOI: 10.1103/PhysRevLett.120.047402

Dipolar excitons in coupled quantum wells (CQW) offer an interesting test bed for studying collective effects of an interacting quantum degenerate system [1,2]. Their relatively light mass, which is smaller than that of a free electron, implies that the necessary conditions for achieving quantum degeneracy can occur already at cryogenic temperatures, and their strong dipole-dipole interaction may give rise to the formation of ordered phases. Extensive attempts have been made over the past two decades to observe these phases and to determine the phase diagram of this system [3–12].

In recent years there is mounting evidence for a phase transition that occurs at low temperatures in this system, yet its nature and thermodynamics remain open questions. Many of the studies are performed in a trap geometry, which confines the excitons to a narrow region around the illuminated spot [13,14] and evidence for condensation is found through photoluminescence (PL) anomalies: The appearance of spontaneous coherence [7], onset of nonradiative recombination ("PL darkening") [9] and large blueshift of the PL energy [10,11]. An alternative approach to study this phase transition uses an open geometry, where photoexcited carriers are free to move away from the illumination spot, and their diffusion is limited only by the mesa boundary. We have recently studied the behavior of indirect excitons in such an open geometry, and found an abrupt phase transition at a critical temperature and excitation power density [12]. The PL separates into two spatial regions, one which consists of electron-hole plasma and another that has a set of properties of a high density liquid.

In this work we investigate this phase transition using spatially resolved PL and resonant Rayleigh scattering (RRS). Measuring the threshold power density as a function of temperature we determine the phase diagram of the system over the temperature range 0.1–4.8 K. Pump probe measurements, in which the liquid is created by a focused pump beam and studied by a much weaker probe, reveal that the liquid is dark and diffuses to large distances away from the illuminated spot, filling the entire area of the mesa at low temperatures. We find that the RRS spectrum narrows significantly and becomes uniform over macroscopic distances at the liquid phase, indicating that the disorder in the sample is effectively screened.

The sample structure is identical to that used in Ref. [12] and consists of two GaAs quantum wells with well widths of 12 and 18 nm, separated by a 3-nm $Al_{0.28}Ga_{0.72}As$ barrier. Top and bottom n-doped layers allow the application of voltage that shifts the energy levels of the wide well (WW) relative to the narrow well (NW) [15]. To create the liquid we apply voltages exceeding -2.4 V and excite the system with a laser diode at energy of 1.590 eV, focused to a Gaussian spot with 22 μm half width at half maximum (HWHM) [16].

Figure 1 shows the evolution of the PL spectrum with power at $T = 0.3$ K and $V = -3.0$ V. At power density levels below threshold the PL spectrum is dominated by the WW direct exciton peak X_{WW} at 1.524 eV [16]. The lower panel shows the corresponding image of the spatial distribution of the total PL intensity from the mesa: A Gaussian profile, reflecting the shape of the illuminating beam, is observed. When the power is increased beyond a threshold power $P_C = 30$ μW, corresponding to a power density of 1.3 W/cm^2, we observe a sudden change in the PL spectrum and spatial distribution: a new broad spectral line Z, appears at 1.518 eV, and a dark ring forms around the center of the beam. This spectral line was identified in Ref. [12] as due to indirect recombination of electrons and

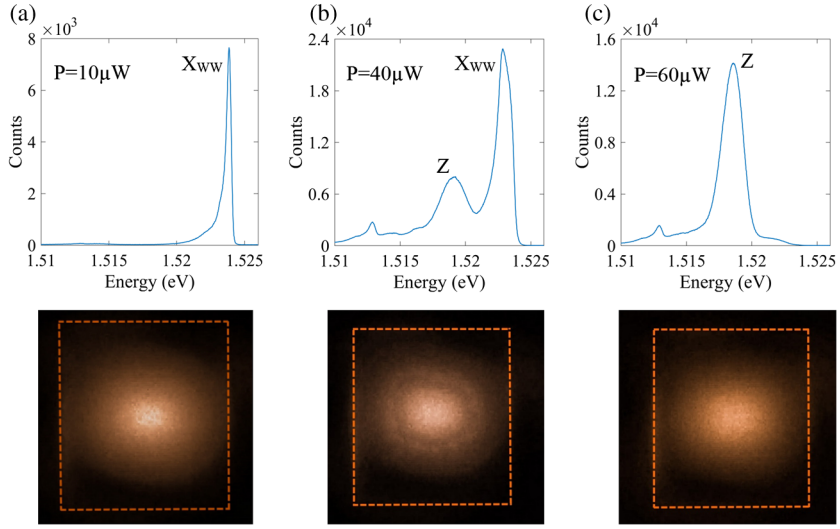

FIG. 1. The upper and lower panels show the PL spectra and PL images, respectively, at different pump powers at a fixed $V_g = -3.0$ V and $T = 0.3$ K. The mesa is 100 μm × 100 μm and is marked by dashed lines. (a) At low power, $P = 10$ μW, the WW direct exciton peak, X_{WW}, is observed and the image is a smooth Gaussian (the low energy shoulder is due to a trion peak). (b) At power above threshold, $P = 40$ μW, a new broad spectral line Z is observed in the spectrum and correspondingly, a dark ring appears in the PL image around the center of the illumination spot. (c) As the power is further increased, $P = 60$ μW, the X_{WW} line disappears and the emission spectrum is dominated by the Z line. Also, the dark boundary disappears in the PL image.

holes in a liquid state, and the dark ring is formed due to the repulsion of the excitons in the gas by the high-density dipoles at the liquid [12]. As the power is further increased the dark ring shrinks in size and eventually disappears. This behavior is robust and remains qualitatively the same as we change the spot size, such that the threshold power density remains at ~ 1 W/cm^2. In the measurements that are described throughout the paper the spot size is kept constant with 22 μm HWHM.

Spatially resolved measurements, where a pinhole of 10 μm diameter is used to resolve the PL, reveal that the Z line appears only at the outer region that surrounds the dark ring, while the X_{WW} line appears in the inner region. Hence, the differences in the relative strength of the X_{WW} and Z peaks in Fig. 1 reflect simply the changes in the relative areas of the inner and outer regions.

We determine the gas-liquid phase diagram by measuring the threshold power P_C as we vary the temperature at constant voltage (blue dots Fig. 2). The direct proportionality between power and carrier density in the gas phase, where recombination is dominated by X_{WW}, implies that we are in fact determining the phase diagram in the carrier density-temperature plane. It is seen that the plane is divided into two regions, a first region of gas only and a second region where liquid appears, with a line of coexistence between them. It is instructive to compare this coexistence line to the Clausius-Clapeyron (C-C) relation, $d\mathcal{P}/dT = L/(T\Delta\nu)$, which describes a general gas-liquid phase transition [18]. Here $\mathcal{P}$ is the gas pressure, L is the latent heat, and Δv is the specific volume change at the transition. In the dipolar exciton gas, the pressure can be expressed as $\mathcal{P} = \alpha n^2$, where n is the exciton gas density and $\alpha = e^2 d/\varepsilon$ (d is the distance between the center of the wells, and ε is the dielectric constant) [19], and Δv can be approximated by n^{-1}. Hence, the C-C equation takes the form $dn/dT = L/(2\alpha T)$. The inset of Fig. 2 shows the resulting $L(T)$ obtained from the experimental data by taking the value of $T\Delta P_C/\Delta T$ at each temperature (in units of L_0 defined below). Two regimes can be clearly identified: (i) $T \lesssim 1.1$ K where the latent heat exhibits a linear dependence on T, extrapolating to $L \approx 0$ at $T = 0$ K;

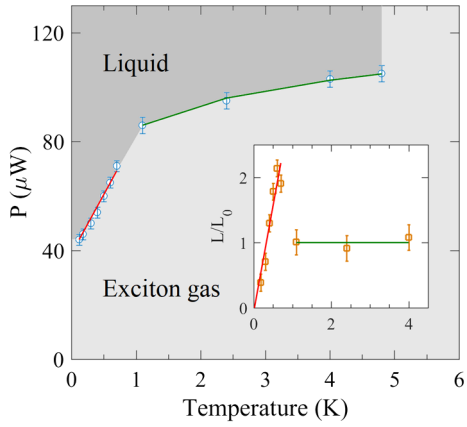

FIG. 2. The phase diagram of the system obtained by measuring the threshold power P_C as a function of temperature at $V = -2.6$ V. The inset shows the latent heat L as a function of temperature using the C-C equation. The solid lines in the main figure are fit to the integrated C-C equation using the values of L from the inset.

(ii) $1.1 \lesssim T < 4.8$ K where the latent heat is constant and equals L_0. (The transition temperature between the two regimes is in the vicinity of 1.1 K but was not determined precisely.) With these assumptions the C-C equation could be easily integrated, and fitted to the experimental data (solid lines in Fig. 2). We confirm the validity of this phase diagram by repeating this measurement under different conditions, where the pump energy is tuned to 1.530 eV, such that carriers are excited in the WW only. A similar phase diagram, with lower threshold power, is obtained. Remarkably, the latent heat exhibits exactly the same behavior with two temperature regimes [16].

We note that a linear dependence of L on temperature is expected for a Bose-Einstein condensation (BEC) transition [20]. Indeed, this is the predicted behavior of dipolar excitons at low temperatures [21]. Hence, our findings could be considered as an indication that the exciton liquid at low temperatures undergoes a BEC. We can estimate the value of L_0 using the measured critical density of the gas at 1.5 K, $\sim 2 \times 10^{10}$ cm^{-2}, and $d = 18$ nm [12]. The resulting latent heat per particle is $L_0 \approx 1$ meV, consistent with the interaction energy scale of the dipolar exciton liquid, and similar to that of ^{4}He [22].

We turn now to describe our RRS measurements. It is well known that RRS is an insightful probe of critical phenomena because of its sensitivity to the disorder in the sample, which often changes near a critical point [23,24]. We perform our measurements in a pump-probe configuration, creating the liquid by the laser diode pump and measuring the scattered intensity of a much weaker Ti: sapphire probe, tuned to the NW exciton resonance. We use the fact that the RRS signal should be strongly enhanced at an exciton resonance, and its linewidth is a measure of the disorder in the sample [25,26]. Hence, the RRS of the NW direct exciton can serve as an effective probe for the changes induced by the liquid.

First, we study the behavior at low power density and voltage, when tunneling from the WW to the NW is inhibited. The RRS signal is easily detected in this range as a sharp spectral line at the laser frequency, riding on the broad NW PL spectrum, and its line shape is obtained by tuning the laser frequency and measuring the scattered intensity. A typical spectrum is depicted by the dashed line in Fig. 3(a). Its spectral width, $\Gamma = 0.3$ meV, remains unchanged in the relevant temperature range, 0.1–5 K, and manifests the static disorder in the sample due to well width and alloy fluctuations. As we increase the voltage the NW is populated by electrons that tunnel from the WW, the NW luminescence becomes trionic, and the RRS signal gradually diminishes, such that above -3.0 V it is undetectable [16].

This behavior changes as we cross the transition threshold, and a strong RRS signal abruptly appears. The open circles in Fig. 3(a) show the RRS spectrum at $T = 0.6$ K when the pump power is set to be above P_C. We find

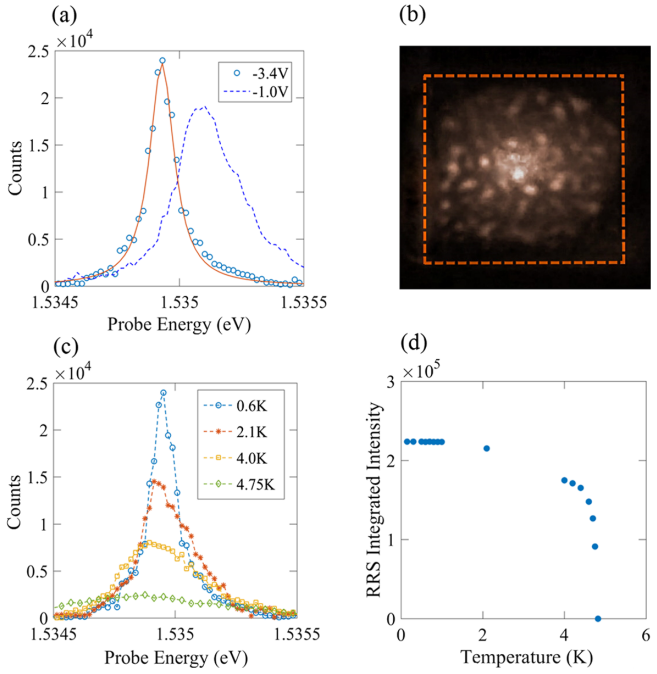

FIG. 3. RRS measurements with overlapping pump (50 μW) and probe (5 μW) beams at $V = -3.4$ V. (a) The measured RRS spectrum at $T = 0.6$ K (blue circles) and a Lorentzian fit (solid red line). The dashed line shows the RRS spectrum at preliquid voltage, $V = -1$ V. (b) Image of the mesa emission (RRS + PL) when the probe energy is set at the NW exciton peak and $T = 0.6$ K. The spotty RRS pattern is clearly observed. (c) The RRS spectra at several temperatures below T_C. (d) The RRS integrated intensity as a function of temperature. It is seen that it is constant at $T < 1.1$ K, then changes by less than 20% at $1.1 < T < 4$ K, and rapidly diminishes towards T_C.

that the spectrum becomes significantly narrower, $\Gamma = 0.12$ meV, and exhibits a strong temperature dependence [Fig. 3(c)], in contrast to the behavior below threshold. The two temperature regimes identified in the phase diagram (Fig. 2) are well manifested in the temperature dependence of the RRS spectrum. We find that at $T \lesssim 1.1$ K the RRS spectrum remains unchanged as we vary the temperature, keeping the same width and height, and it rapidly broadens and weakens at $1.1 < T < 4.8$ K. As we approach $T_C = 4.8$ K [27] the RRS signal drops sharply, and cannot be observed at any power or voltage above that temperature [Figs. 3(c) and 3(d)].

The solid line in Fig. 3(a) is a fit of the measured points at 0.6 K to a Lorentzian: A good agreement is obtained, suggesting that the excitonic line is predominantly homogeneously broadened at $T \lesssim 1.1$ K [16]. Since the RRS signal is collected from the entire probe area, this narrow and symmetric line implies that the static disorder potential in the NW is effectively screened at the liquid phase. This conclusion is corroborated by spatially resolved measurements. Figure 3(b) shows an image of the mesa emission when the probe frequency is set at the NW exciton peak. It is seen that the RRS signal comes mainly from bright spots

at fixed locations on the mesa. We find that while the intensity of the spots varies, their spectra are rather uniform. Analysis of the scattering from spots that are located tens of μm away from one another reveals that their spectral widths are similar and the variation between their peak energy is smaller than the laser spectral resolution, 20 μeV [16]. Such a uniform RRS spectral signal from remote locations implies that the energy landscape seen by the NW excitons is nearly flat over macroscopic distances.

Screening of the disorder potential by dipolar exciton liquid was predicted and calculated in several theoretical works [28,29]. It was shown that the repulsive dipole-dipole interaction pushes the excitons to the local potential minima, and thereby changes their density profile. This generates a smoother potential that is the sum of the random potential and the Hartree repulsion by the localized excitons. In the quantum degenerate regime this screening is expected to be strongly enhanced, such that a disorder potential of 0.5 meV amplitude should be practically screened out for densities exceeding 10^{10} cm^{-2} [28]. Our findings are to our knowledge the first direct observation of this screening effect.

To obtain further insight into this screening effect we study the spatial dependence of the RRS intensity. We find that at intermediate pump power levels, $P \sim 40$ μW, the RRS signal exhibits spatial phase separation, similarly to the PL signal. This is demonstrated in Fig. 4(a), where the stark contrast between the two regions and the dark phase boundary are clearly observed. It is seen that strong RRS is obtained only at the outer parts of the illuminated area, confirming the global nature of the liquid formation. We then shift the probe beam to the side of the mesa and examine the RRS signal away from the pump beam [Fig. 4(b)]. Remarkably we find that the RRS signal in this area is similarly intense and exhibits the same behavior as in the main beam: Abrupt enhancement of intensity as the pump power crosses threshold, narrow linewidth and a spotty pattern. This behavior is found as we position the probe beam anywhere in the mesa, proving that the liquid diffuses beyond the pump region into the whole area of the mesa.

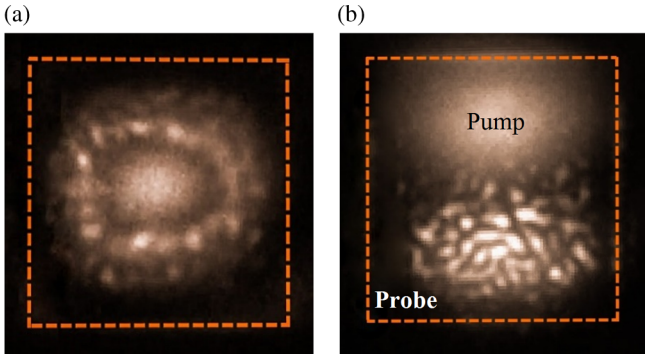

FIG. 4. Images of the mesa emission (RRS + PL) for probe excitation in resonance with the NW exciton at −3.0 V and $T = 0.6$ K. (a) Overlapping pump and probe at intermediate pump power (40 μW), where phase separation occurs. (b) Non-overlapping pump (at the top) and probe (at the bottom) at high pump power (60 μW). The orange dashed square marks the mesa.

We find that the liquid diffusion *decreases* with increasing temperature: While at 0.6 K the RRS intensity (averaged over the area of the probe) remains constant as we shift the probe throughout the mesa, at 4 K it drops by a factor of 5 between overlapping [Fig. 4(a)] and non-overlapping [Fig. 4(b)] configurations. This unique temperature dependence is a manifestation of the repulsive interaction E_{int}, which characterizes the dipolar exciton liquid, and enhances the diffusion constant by a large factor E_{int}/T [28,30]. In the quantum regime this diffusion constant is expected to be further increased, by another factor of $\exp(T_C/T)$ [28], allowing the excitons to cross macroscopic distances within the liquid lifetime [12].

In concluding, we wish to return to the PL measurements, this time performed in a pump-probe configuration, where we set the pump and probe energy at 1.590 eV, and collect the probe PL from the area marked by the small rectangle in Fig. 5(a). We find that the PL spectrum of the probe changes as we switch on the pump and set its power to be above P_C, in a similar manner to the changes observed for the pump PL [Fig. 5(b)]. Shifting the probe beam

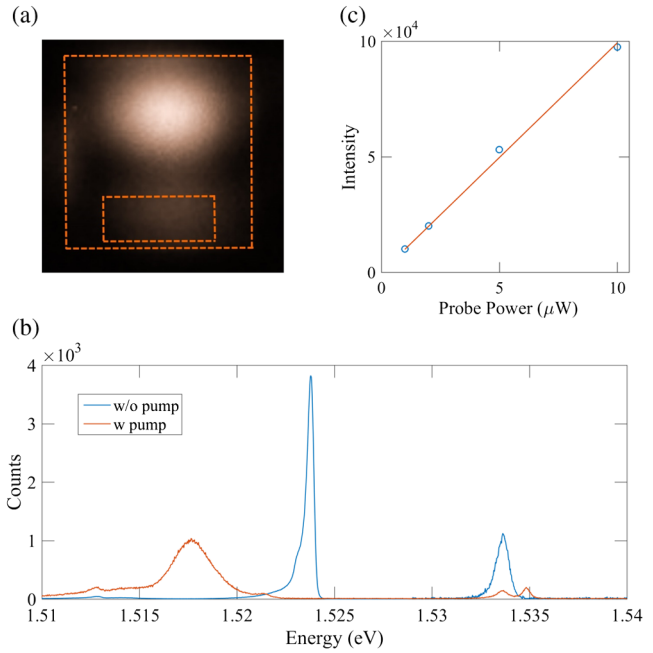

FIG. 5. Two-beam PL measurements at $P = 50\,\mu$W, $V = -3.0$ V, $T = 0.6$ K. (a) A typical setting of the pump (top) and probe (bottom) experiment. The small rectangle marks the area from which PL is collected. (b) The PL spectrum from the WW and NW without (blue) and with (red) the pump beam. The indirect exciton appears as a weak peak at 1.500 eV, outside the range of this figure [16]. (c) The integrated PL intensity from the marked area as a function of probe power when the pump is switched on.

around reveals that the liquid spectrum is observed throughout the mesa, yet we could detect light emission only when the liquid is probed by an exciting beam. This is demonstrated in Fig. 5(c), which shows the Z line intensity as a function of probe power. It is seen that the PL intensity extrapolates to approximately zero when the probe power vanishes. We conclude that the Z line is not due to recombination of the liquid carriers, as we postulated in Ref. [12], but rather, recombination in the presence of the liquid. It is plausible to assume that it is due to recombination of carriers in the NW and WW which have not relaxed into the condensate with carriers having opposite charge in the condensate.

Evidence for the nonradiative nature of the dipolar exciton liquid was recently reported in Ref. [11]. It was suggested that the excitons condense in a "dark" state, consisting of electrons and holes in parallel spin configuration that cannot couple to light. This state is lower in energy than that of the bright exciton, and should therefore be the ground state for BEC [31]. One would expect, however, scattering mechanisms to give rise to some emission, turning the condensate to become "gray" [32]. We find no clear evidence for such emission within our detection limit, set by the Gaussian tail of the pump [16]. Further experiments are needed to provide explanation for the origin of this effect.

This work was supported by the Israeli Science Foundation under the Grant No. 557/16.

*Corresponding author.
ibj@weizmann.ac.il

[1] D. W. Snoke, Adv. Condens. Matter Phys. **2011**, 938609 (2011).
[2] M. Combescot, R. Combescot, and F. Dubin, Rep. Prog. Phys. **80**, 066501 (2017).
[3] L. V. Butov, A. C. Gossard, and D. S. Chemla, Nature (London) **418**, 751 (2002).
[4] D. Snoke, S. Denev, Y. Liu, L. Pfeiffer, and K. West, Nature (London) **418**, 754 (2002).
[5] A. V. Gorbunov and V. B. Timofeev, JETP Lett. **84**, 329 (2006).
[6] A. A. High, J. R. Leonard, A. T. Hammack, M. M. Fogler, L. V. Butov, A. V. Kavokin, K. L. Campman, and A. C. Gossard, Nature (London) **483**, 584 (2012).
[7] A. A. High, J. R. Leonard, M. Remeika, L. V. Butov, M. Hanson, and A. C. Gossard, Nano Lett. **12**, 2605 (2012).
[8] M. Alloing, M. Beian, M. Lewenstein, D. Fuster, Y. Gonzalez, L. Gonzalez, R. Combescot, M. Combescot, and F. Dubin, Europhys. Lett. **107**, 10012 (2014).
[9] Y. Shilo, K. Cohen, B. Laikhtman, K. West, L. Pfeiffer, and R. Rapaport, Nat. Commun. **4**, 2335 (2013).
[10] J. K. Wuenschell, N. W. Sinclair, Z. Voros, D. W. Snoke, L. N. Pfeiffer, and K. W. West, Phys. Rev. B **92**, 235415 (2015).
[11] K. Cohen, Y. Shilo, K. West, L. Pfeiffer, and R. Rapaport, Nano Lett. **16**, 3726 (2016).
[12] M. Stern, V. Umansky, and I. Bar-Joseph, Science **343**, 55 (2014).
[13] D. W. Snoke, Y. Liu, Z. Voros, L. Pfeiffer, and K. West, Solid State Commun. **134**, 37 (2005).
[14] A. Gartner, L. Prechtel, D. Schuh, A. W. Holleitner, and J. P. Kotthaus, Phys. Rev. B **76**, 085304 (2007).
[15] We did not form side contacts as in Ref. [12], thus eliminating their potential role as nucleation sites.
[16] See Supplemental Material at http://link.aps.org/supplemental/10.1103/PhysRevLett.120.047402 for description of the sample structure and methods, as well as supporting experimental results, which includes Ref. [17].
[17] R. Rapaport, G. Chen, D. Snoke, S. H. Simon, L. Pfeiffer, K. West, Y. Liu, and S. Denev, Phys. Rev. Lett. **92**, 117405 (2004).
[18] L. D. Landau and E. M. Lifshitz, *Statistical Physics Part 1* (Pergamon Press, Oxford, 1988).
[19] R. A. Suris, J. Exp. Theor. Phys. **122**, 602 (2016).
[20] K. Huang, *Statistical Mechanics,* 2nd ed. (John Wiley & Sons, New York, 1988).
[21] B. Laikhtman and R. Rapaport, Phys. Rev. B **80**, 195313 (2009).
[22] R. A. Erickson and L. D. Roberts, Phys. Rev. **93**, 957 (1954).
[23] H. Z. Cummins and A. P. Levanyuk, *Light Scattering near Phase Transitions* (North Holland Publishing Co., Amsterdam, New York, Oxford, 1983).
[24] S. Luin, V. Pellegrini, A. Pinczuk, B. S. Dennis, L. N. Pfeiffer, and K. W. West, Phys. Rev. Lett. **97**, 216802 (2006).
[25] J. Hegarty, M. D. Sturge, C. Weisbuch, A. C. Gossard, and W. Wiegmann, Phys. Rev. Lett. **49**, 930 (1982).
[26] S. Haacke, Rep. Prog. Phys. **64**, 737 (2001).
[27] The transition temperature was reported to be at 4.7 K in Ref. [12]. Refined measurements revealed that it occurs at 4.8 K.
[28] A. L. Ivanov, Europhys. Lett. **59**, 586 (2002).
[29] R. Zimmermann, Solid State Commun. **134**, 43 (2005).
[30] M. Stern, V. Garmider, E. Segre, M. Rappaport, V. Umansky, Y. Levinson, and I. Bar-Joseph, Phys. Rev. Lett. **101**, 257402 (2008).
[31] M. Combescot, O. Betbeder-Matibet, and R. Combescot, Phys. Rev. Lett. **99**, 176403 (2007).
[32] R. Combescot and M. Combescot, Phys. Rev. Lett. **109**, 026401 (2012).